Structural and energetic properties of sodium clusters

V. Tevekeliyska[a], Y. Dong[b], M. Springborg[c], and V.G. Grigoryan[d]

Physical and Theoretical Chemistry, University of Saarland, 66123 Saarbrücken, Germany

Abstract. In this work we present results from a theoretical study on the properties of sodium clusters. The structures of the global total-energy minima have been determined using two different methods. With the parameterized density-functional tight-binding method (DFTB) combined with a *genetic-algorithm* we investigated the properties of Na_N clusters with cluster size up to 20 atoms, and with our own *Aufbau/Abbau* algorithm together with the embedded-atom method (EAM) up to 60 atoms. The two sets of results from the independent calculations are compared and a stability function is studied as function of the cluster size. Due to the electronic effects included in the DFTB method and the packing effects included in the EAM we have obtained different global-minima structures and different stability functions.

PACS. 36.40.-c Atomic and molecular clusters – 61.46.Bc Clusters

1 Introduction

Na_N clusters have for a long time constituted one of the prototypes of clusters. The fact that each atom has only one valence electron and that the interatomic interactions to some extend are undirectional has made Na_N clusters a popular system. Systematical theoretical studies have been done with different approaches. Some of these are based on the *jellium model*, that is often used to describe the delocalized electrons in metallic clusters [1,2]. One major outcome of the *jellium model* in its simple spherical version is the understanding of the *magic numbers*. Indeed, the most intense peaks occurring in mass spectra for $N = 2, 8, 18, 20, 34, 40, 58$, etc., were explained as being due to electronic shell closure directly resulting from completing the filling of electronic shells. One major advantage of this model is that structural degrees of freedom are largely abandoned.

Alternatively, both structural and electronic degrees of freedom can be treated within a Hückel model [3,4]. For $N \leq 20$, this model predicts a clear even-odd staggering, with the most stable clusters found for $N = 8$ and 14, and slightly less stable for $N = 6, 10$, and 16. A very accurate treatment of the electronic degrees of freedom is provided by first-principles calculations. When combining these with molecular-dynamics simulations, structural degrees of freedom can also be determined, although it is known that molecular-dynamics simulations not are the optimal methods for unbiased structure optimizations.

[a] e-mail: v.tevekeliyska@mx.uni-saarland.de
[b] e-mail: y.dong@mx.uni-saarland.de
[c] e-mail: m.springborg@mx.uni-saarland.de
[d] e-mail: vg.grigoryan@mx.uni-saarland.de

Such calculations have found an overall support for the *jellium model* [5,6].

However, special-purpose methods for unbiased structure optimizations that have been developed during the last decade have, for Na_N clusters, so far been used only in combination with total-energy methods that do not include explicitly electronic degrees of freedom. In order to study the role of the electronic orbitals, we shall here extend the earlier studies on unbiased structure optimization by using one method that includes the electronic degrees of freedom directly and compare with the results of another method where the electronic degrees of freedom are not directly included.

2 Computational methods

As one method we used the density-functional tight-binding method (DFTB) that is based on the density-functional theory (DFT) of Hohenberg and Kohn [7] in the formulation of Kohn and Sham [8], and developed by Seifert and coworkers [9–11]. According to this method the relative total energy of a given compound with a given structure is written as the difference in the orbital energies of the compound minus those of the isolated atoms, $\sum_i \epsilon_i - \sum_j \sum_k \epsilon_{jk}$ (with j being an atom index and k an orbital index), augmented with pair potentials, $\sum_{k \neq l} U_{kl}(|\boldsymbol{R}_k - \boldsymbol{R}_l|)$ (with $\boldsymbol{R}_k$ being the position of the kth atom). For the determination of the global total-energy minimum we have used a so called *genetic algorithm*. There are different approaches for *genetic algorithms* [12–16]. In all approaches, from a set of structures we generate new ones through cutting and pasting the

original ones. Out of the total set of old and new clusters those with the lowest total energies are kept, and this process is repeated until the lowest total energy is unchanged for a large number of generations.

For the other set of calculations we have used a combination of the embedded-atom method model constructed by Chantasiriwan et al. [17], and our own *Aufbau/Abbau* method for the determination of the global total-energy minimum [18–20]. In reference [17] the higher-order elasticity of cubic metals is investigated in the framework of the embedded-atom method, and formulas are given for computing the second- (SOEM) and third-order elastic moduli (TOEM) in general EAM formulations. However, it was necessary to correct the potential developed by Chantasiriwan et al. For our correction we added to this potential, $\phi(r)$, an additional term with two new constants, $c = 82$ and $d = 2.4$ (in a.u.), giving, for $r < d$, $\phi_{corr}(r) = \phi(r) + c(r/d - 1)^4$, whereas $\phi(r)$ is unchanged for $r > d$. Our own *Aufbau/Abbau* method [18–20], used for optimizing the structures is based on simulating experimental conditions, where clusters grow by adding atom by atom to the core. By repeating this process many times and in parallel also removing atoms from larger clusters, we have identified the structures of the lowest total energy.

3 Results

3.1 Global total-energy structures obtained with DFTB

Figure 1 shows the structures of the clusters with up to twenty atoms. For the very small systems we found a planar ground state structure and a structural transition 2D–3D at Na_7. For Na_3 we obtained a linear structure with $D_{\infty h}$ symmetry, in contrast to the C_{2v} symmetry of [3,21–24]. All of these studies found the isoceles triangle as the equilibrium geometry of the Na_3 trimer. The linear structure here is due to the strong Jahn-Teller distortion, which usually is responsible for the deviation from the equilateral triangle geometry. For the tetramer a rhombic equilibrium geometry with D_{2h} symmetry was found. The sides of the rhombus are larger than the small diagonal, in agreement with the results from [3,23,24], while in other works all distances were found to be equal, e.g. [25]. The equilibrium geometry of Na_5 is planar with an almost trapezoidal shape (C_{2v}) formed by three slightly distorted equilateral triangles. Poteau et al. [21,22] found also the triangular bipyramid (C_{2v} symmetry) as a higher-lying isomer. The triangular shape of Na_4 and Na_6 and their stability (see Fig. 4) correspond to the results of Reimann et al. [26], who found that clusters with triangular or tetrahedral shapes have a strong electronic-shell structure and enhanced stability.

However, the different studies do not agree upon at which cluster size the 2D–3D structural transition occurs. According to the Hückel studies of Poteau et al. [21,22] and Wang et al. [3] the ground state of Na_6 is the pentagonal pyramid with C_{5v} symmetry and the planar structure is the second-lowest isomer [21] with a very small energy difference. The ab initio results of Martins et al. [23]
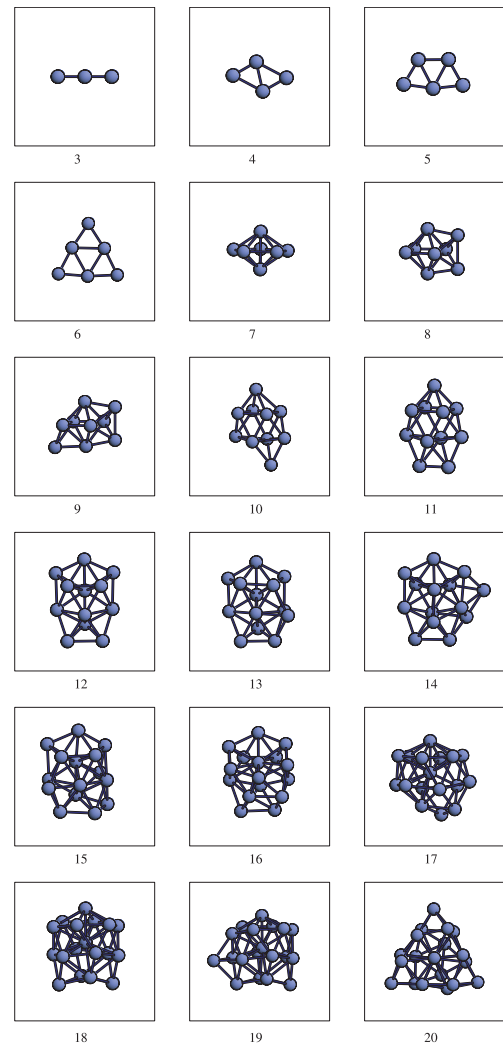

Fig. 1. Structures of the global total-energy minima obtained with the DFTB method. Below each structure is given the number of atoms the clusters consist of.

and Röthlisberger et al. [5] gave also the pentagonal pyramid as a ground state of Na_6, while Bonačić-Koutecký et al. [24] found that the 2D–3D transition to occur at Na_7 so that the equilibrium geometry of Na_6 is planar, formed by a central equilateral triangle surrounded by three isoceles triangles, with the D_{3h} symmetry in agreement with our results and with those of Reimann et al. [26]. For charged clusters, Martins et al. [23] found that the Na_6^+ is the first 3D structure and with a very low symmetry (C_s). Na_5^+, in agreement with the theoretical and experimental results of Moseler and coworkers [27], has a planar geometry, where two isoceles triangles with a common apex can rotate almost freely. In contrast, Wang et al. [3] found that the 2D–3D transition occurs at Na_5^+.

For Na_7 we found the pentagonal bipyramid to be the ground state structure (D_{5h} symmetry), in agreement with all previous calculations. Na_7 is the smallest cluster that incorporates the fivefold symmetry axis and can be taken as a step in the pentagonal cluster growth. The equilibrium geometry of Na_8 has a rather compact structure with

D_{2d} symmetry, as also found in [3,5,23]. This dodecahedral structure corresponds to the optimum arrangements of spheres and is known as the *Bernal* structure. Bonačić-Koutecký et al. [24], and Poteau and Spiegelmann [21,22] obtained the highly symmetric tetrahedron (T_d) as the ground state of Na_8. Low-symmetric structures are found for the clusters with 9–20 atoms, where the point groups C_1, C_2, and C_s dominate. Most of our results are in good agreement with the global-minima structures from Poteau et al. [22]. The Na_{13} cluster has C_2 symmetry in our work, whereas the C_1 symmetry is obtained in references [21,22]. As expected, the icosahedral structure does not appear as a stable structure due to the Jahn-Teller effect. In contrast, Martins et al. [23] obtained the equilibrium geometry of Na_{13} by studying a few symmetrical distortions of the cuboctahedron and found a structure with D_{4h} symmetry. For the *magic clusters* with $N = 18$ and 20 we found the C_{2v} and C_3 point groups, respectively. The same structure for Na_{20} with the same symmetry as ours is found in reference [22], and the lowest energy isomer of Na_{18} has the C_{5v} symmetry. According to the ab initio molecular dynamics studies of Röthlisberger et al. [5] the clusters prefer the pentagonal growth, which is dominant for Na_{18} and Na_{20} and in contrast to the other results.

In total, it is clear that methods that include electronic degrees of freedom tend to find low-symmetry structures for even small values of N, although it shall be remembered that both small changes in the relative total energies of different isomers may lead to a change in the energetic ordering of those, and that small structural changes may appear as strong symmetry changes.

3.2 Global total-energy structures obtained with EAM

Due to the packing effects included in the embedded-atom method (EAM) we obtained more compact structures with higher symmetry than with the DFTB method. In Figure 2 we show global minima structures of Na_N clusters with up to 20 atoms. We shall compare our results with those of other studies based on unbiased structure optimizations using simple descriptions of the interatomic interactions, i.e., studies based on the Gupta and the Murrell-Mottram potential [28]. Like the embedded-atom method, these two potentials do not take into account electronic effects.

Only for Na_3 we found a planar geometry with the D_{3h} symmetry, and the same was found also in [28]. The tetrahedral structure for Na_4 (T_d), the trigonal bipyramid for Na_5 (D_{3h}), the octahedron for Na_6 (O_h), the pentagonal bipyramid for Na_7 (D_{5h}), and the bisdisphenoid for Na_8 (D_{2d}) are also in good agreement with the results from reference [28]. From Na_9 (C_{2v}) to Na_{13} (I_h) and from Na_{14} (C_{2v}) to Na_{19} (D_{5h}) it can be seen how the high symmetrical icosahedron, Na_{13}, and the double icosahedral structure of Na_{19} are formed.

Some of the larger *magic clusters* are shown in Figure 3. The structures of Na_{23} (D_{3h}), Na_{26} (T_d), Na_{45} (C_1), and Na_{55} (I_h) are in good agreement with [28] and as
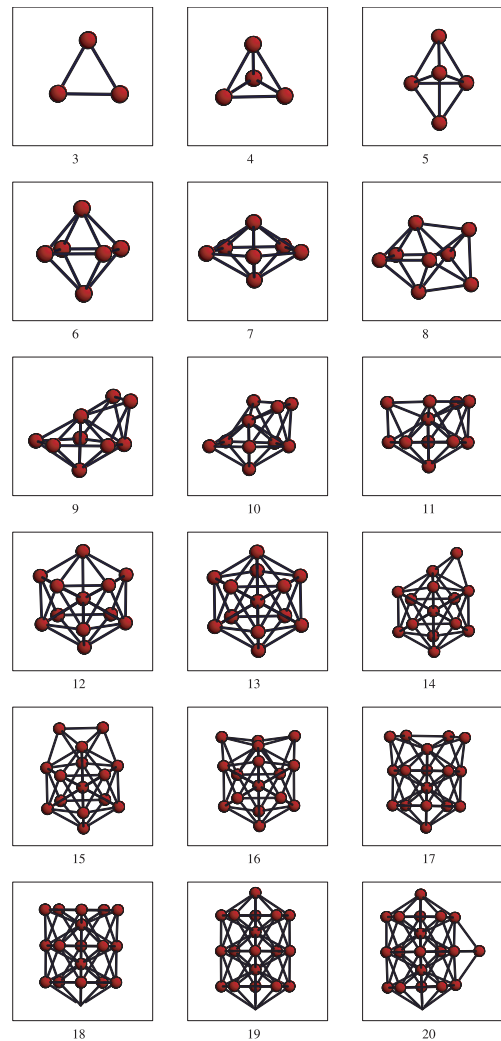

Fig. 2. Structures of the global total-energy minima obtained with the EAM method. Below each structure is given the number of atoms the clusters consist of.
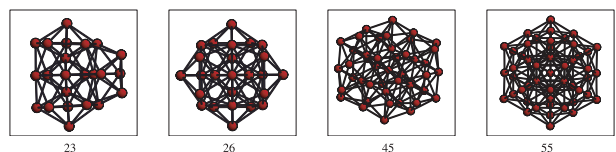

Fig. 3. Structures of the larger magic Na_N clusters obtained with the EAM method. Below each structure is given the number of atoms the clusters consist of.

above correlation between high symmetry and high stability of the cluster is observed.

3.3 Energetic stability

From the energetic properties we investigated the stability function of the clusters, defined as $E_{tot}(N+1) + E_{tot}(N-1) - 2E_{tot}(N)$, and shown in Figure 4. This has maxima for particularly stable clusters. The upper panel shows the results from the DFTB calculations and the lower one the results from the EAM method.
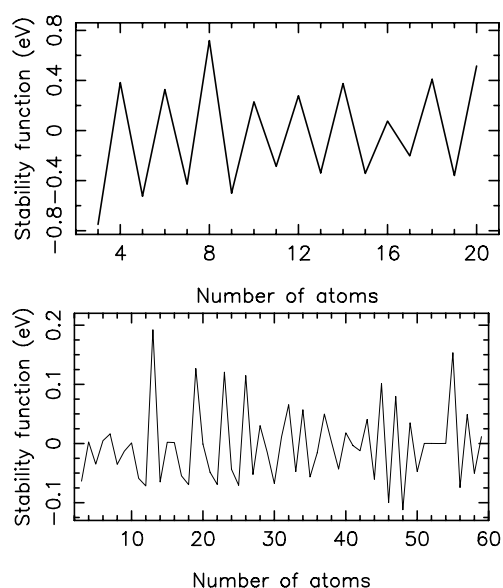
Fig. 4. The two stability functions as function of the size of the clusters (in eV).

agreement with previous investigations. Therefore, our study, based on an unbiased structure optimization, confirms earlier findings that an accurate inclusion both of electronic effects and of structural effects even for clusters of simple metals are important in an accurate description of the properties of these systems.

The DFTB stability function shows that the even-numbered clusters tend to be more stable than the odd-numbered ones, and the most pronounced peaks occur for $N = 8, 18, 20$, i.e. for the structures with closed electronic shell for the spherical *jellium model.*

As expected, due to the packing effects considered in the embedded-atom method, we obtained here *magic clusters* both with even and with odd number of atoms, for example: Na_{13}, Na_{19}, Na_{23}, Na_{26}, Na_{45}, Na_{47}, Na_{55}. There is also here a correlation between high symmetry and high stability of the cluster. The most stable clusters are highly symmetrical.

Furthermore, it is clear that the *magic clusters* that were found in the DFTB calculations show an overall agreement with those of the Hückel calculations (that we mentioned in the introduction) although the finer details of the total-energy variations differ.

4 Conclusions

In the present work we have studied some of the properties of sodium clusters using two different methods. The embedded-atom method provided more compact clusters with higher symmetry, while Jahn-Teller distorted structures of lower symmetry are found with the density-functional tight-binding method. A large number of particularly stable clusters was identified. The odd-even character of the DFTB stability function oscillations showed that the even-numbered clusters tend to be more stable than the odd-numbered ones. In contrast to this, the EAM calculations identify magic clusters with both even and odd number of atoms. Moreover, in the EAM studies most of the stable clusters possess high symmetry.

Finally, the two different sets of results obtained with the two different computational methods are in good

References

1. W.D. Knight, K. Clemenger, W.A. de Heer, W.A. Saunders, M. Chou, M.L. Cohen, Phys. Rev. Lett. **52**, 2141 (1984)
2. W. Ekardt, Phys. Rev. Lett. **52**, 1925 (1984)
3. Y. Wang, T.F. George, D.M. Lindsay, A.C. Beri, J. Chem. Phys. **86**, 3493 (1987)
4. A. Yoshida, T. Døssing, M. Manninen, J. Chem. Phys. **101**, 3041 (1994)
5. U. Röthlisberger, W. Andreoni, J. Chem. Phys. **94**, 8129 (1991)
6. M. Moseler, B. Huber, H. Häkkinen, U. Landman, G. Wrigge, M. Astruc Hoffmann, B. v. Issendorff, Phys. Rev. B **68**, 165413 (2003)
7. P. Hohenberg, W. Kohn, Phys. Rev. B **136**, 864 (1964)
8. W. Kohn, L.J. Sham, Phys. Rev. A **140**, 1133 (1965)
9. G. Seifert, R. Schmidt, New J. Chem. **16**, 1145 (1992)
10. D. Porezag, Th. Frauenheim, Th. Köhler, G. Seifert, R. Kaschner, Phys. Rev. B **51**, 12947 (1995)
11. G. Seifert, D. Porezag, Th. Frauenheim, Int. J. Quant. Chem. **58**, 185 (1996)
12. D.M. Deaven, K.M. Ho, Phys. Rev. Lett. **75**, 288 (1995)
13. J.R. Morris, D.M. Deaven, K.M. Ho, Phys. Rev. B **75**, R1740 (1996)
14. J.A. Niesse, H.R. Mayne, Chem. Phys. Lett. **261**, 576 (1996)
15. C. Roberts, R.L. Johnston, N.T. Wilson, Theor. Chem. Acc. **104**, 123 (2000)
16. B. Hartke, Chem. Phys. Lett. **240**, 560 (1995)
17. S. Chantasiriwan, F. Milstein, Phys. Rev. B **53**, 14080 (1996)
18. V.G. Grigoryan, M. Springborg, Phys. Chem. Chem. Phys. **3**, 5125 (2001)
19. V.G. Grigoryan, M. Springborg, Chem. Phys. Lett. **375**, 219 (2003)
20. V.G. Grigoryan, M. Springborg, Phys. Rev. B **70**, 205415 (2004)
21. R. Poteau, F. Spiegelmann, Phys. Rev. B **45**, 1878 (1992)
22. R. Poteau, F. Spiegelmann, J. Chem. Phys. **98**, 6540 (1993)
23. J.L. Martins, J. Buttet, R. Car, Phys. Rev. B **31**, 1804 (1985)
24. V. Bonačić-Koutecký, P. Fantucci, J. Koutecký, Phys. Rev. B **37**, 4369 (1988)
25. F. Spiegelmann, D. Pavolini, J. Chem. Phys. **89**, 4954 (1988)
26. S.M. Reimann, M. Koskinen, H. Häkkinen, P.E. Lindelof, M. Manninen, Phys. Rev. B **56**, 12147 (1997)
27. M. Moseler, H. Häkkinen, U. Landman, Phys. Rev. Lett. **87**, 053401-1 (2001)
28. The Cambridge Cluster Database, http://www-wales.ch.cam.au.uk/CCD.html